



HAL
open science

Effect of coating on the hygric performance of a hemp concrete wall

Yacine Aït Ouméziane, Sophie Moissette, Marjorie Bart, Christophe Lanos

► **To cite this version:**

Yacine Aït Ouméziane, Sophie Moissette, Marjorie Bart, Christophe Lanos. Effect of coating on the hygric performance of a hemp concrete wall. 5th IBPC, May 2012, Kyoto, Japan. pp.109-116. hal-00801140

HAL Id: hal-00801140

<https://hal.science/hal-00801140>

Submitted on 15 Mar 2013

HAL is a multi-disciplinary open access archive for the deposit and dissemination of scientific research documents, whether they are published or not. The documents may come from teaching and research institutions in France or abroad, or from public or private research centers.

L'archive ouverte pluridisciplinaire **HAL**, est destinée au dépôt et à la diffusion de documents scientifiques de niveau recherche, publiés ou non, émanant des établissements d'enseignement et de recherche français ou étrangers, des laboratoires publics ou privés.

Effect of coating on the hygric performance of a hemp concrete wall

Yacine Aït Ouméziane ¹, Sophie Moissette ¹, Marjorie Bart ¹ and Christophe Lanos ¹

¹ UEB, INSA Rennes, LGCGM Laboratoire de Génie Civil et de Génie Mécanique, Rennes, France

Keywords: building material, HAM modelling, hysteresis, hemp concrete, coating

ABSTRACT

Constructions built with environmentally friendly materials like hemp concrete know currently a real development thanks to their low environmental impact and their interesting thermo-hydric properties. Their porous structure presents lots of advantages in terms of life quality compared with usual concretes. An experimental facility is designed to measure temperature and relative humidity within a hemp concrete wall (30 cm thick) submitted to climatic solicitations. This facility provides a set of experimental data suited for benchmarking a 1D HAM model.

In the present work, the wall is submitted to relative humidity gradient under almost isothermal conditions. Comparisons between numerical and experimental data are performed. The results indicate that the use of main wetting curve is suited to describe the storage capacity of the material. However the use of hysteresis modelling is able to improve the description of drying stages.

The hydro-thermal properties of the same wall coated on one side with traditional hemp lime render are then investigated numerically. The coating effect on relative humidity distributions is analysed. The ability of the coating to regulate moisture is pointed out.

1. Introduction

In the context of sustainable development, one of the concerns in building construction is the choice of environmentally friendly and healthy materials. Indeed, it has some impacts on exhaustion of natural resources, energy consumption, polluting emission, etc... Hemp concrete (hemp and lime mortar) is a vapour permeable and highly hygroscopic material more and more studied (Samri 2008, Evrard 2008). The use of such material moderates indoor humidity and improves indoor air quality.

In order to predict the hygrothermal behaviour of this material, a collaborating project with industrial partners is lead and experimental tests and numerical studies are investigated.

In this paper, a 1D numerical model is presented and experimental data recorded on a hemp concrete wall are described. Thus, numerical and experimental results are compared. A sensitivity study of the hygrothermal parameters is presented inducing a reflexion about the use of hysteresis model to describe sorption isotherm.

The hydro-thermal properties of the same wall coated with traditional lime render are then investigated numerically. The case study consists of a 30 cm hemp concrete wall covered on one side with hemp lime coating. Two coating thicknesses are studied : 5 cm or 3 cm. Such a configuration is representative of a usual wall for French hemp concrete house. This coating must provide mechanical, acoustic and design qualities but also moisture regulation properties. In order to analyse the ability of the coating to regulate moisture, relative humidity distributions in the wall are studied through numerical results.

2. HAM model

2.1 Constitutive equations

According to Künzle mathematical model (1995), a multi-layered hygrothermal model based on 1D conservation equations for mass and energy is used. The potentials governing heat and mass transfers are the temperature T and the relative humidity φ .

Mass transfers are governed by humidity transport in liquid and vapour forms and by airflow through the structure. Vapour diffusion is given by Fick's law and liquid transport by Darcy's law. Considering 1D configuration, water vapour, water liquid and air flux are written as:

$$\begin{aligned} g_v &= -\left(\delta_p p_{sat} \frac{\partial \varphi}{\partial x} + \delta_p \varphi \frac{dp_{sat}}{dT} \frac{\partial T}{\partial x} \right) + \rho_a rV \\ g_l &= -\left(K_l \rho_w R_{H_2O} \frac{T}{\varphi} \frac{\partial \varphi}{\partial x} + K_l \rho_w R_{H_2O} \ln(\varphi) \frac{\partial T}{\partial x} \right) \\ g_a &= \rho_a V \end{aligned} \quad (1)$$

with δ_p the vapour permeability of the moist material, ρ_a the air density, p_{sat} and p_{atm} respectively the saturated vapour and atmospheric pressures, ρ_w the water density, K the liquid conductivity of the material, R_{H_2O} the vapour perfect gas constant and V the air velocity. The air velocity is expressed as a function of the pressure difference over the wall by using the conservative equation of air.

The governing equation for the moisture flow is written as follows:

$$\begin{aligned} \frac{dw}{d\varphi} \frac{\partial \varphi}{\partial t} &= \frac{\partial}{\partial x} \left(\delta_p p_{sat} \frac{\partial \varphi}{\partial x} + \delta_p \varphi \frac{dp_{sat}}{dT} \frac{\partial T}{\partial x} \right) \\ &- \delta_a \frac{0.622}{p_{atm}} \frac{\Delta P}{e} \left(p_{sat} \frac{\partial \varphi}{\partial x} + \varphi \frac{dp_{sat}}{dT} \frac{\partial T}{\partial x} \right) \\ &+ \frac{\partial}{\partial x} \left(K_l \rho_w R_{H_2O} \frac{T}{\varphi} \frac{\partial \varphi}{\partial x} + K_l \rho_w R_{H_2O} \ln(\varphi) \frac{\partial T}{\partial x} \right) \end{aligned} \quad (2)$$

Heat transfer is carried out by conduction, convection due to the heat transport by air and vapour water and phase change in pores. Considering 1D configuration, conservation equation for heat is written as:

$$\rho_0 C^* \frac{\partial T}{\partial t} = \frac{\partial}{\partial x} \left[\left(\lambda \frac{\partial T}{\partial x} \right) - \left(C_{p_v} T + l_v \right) g_v - C_{p_a} T g_a \right] \quad (3)$$

with ρ_0 the density of the dry material, C_{p_v} and C_{p_a} the specific heat capacity of respectively vapour and air, C^* the equivalent specific heat capacity of the moist material, λ the equivalent specific heat conductivity of the moist material and l_v the latent heat of evaporation.

2.2 Boundary conditions

Considering an air movement directed from inside to outside, the boundary conditions systems is:

$$g_{ext} = \beta_{ext} (p_{ext} - p_{surf}) + \frac{0.622}{p_{atm}} \rho_a V (p_{ext} - p_{surf}) \quad (4)$$

$$g_{int} = \beta_{int} (p_{int} - p_{surf}) \quad (5)$$

$$q_{ext} = h_{ext} (T_{ext} - T_{surf}) + \rho_a C_{p_a} V (T_{ext} - T_{surf}) + l_v g_{ext} \quad (6)$$

$$q_{int} = h_{int} (T_{int} - T_{surf}) + l_v g_{int} \quad (7)$$

with h and β the heat and mass surface coefficients.

2.3 Validation of the model

The governing system of equation is implemented in Matlab. The present model has been benchmarked against the international benchmark HAMSTAD WP2 (Hagentoft 2004). The exercises of this benchmark are suited to assess the performance and accuracy of hygrothermal model in one dimensional configuration for multi-layered wall submitted to relative humidity, temperature or total pressure gradient. The performances of the model against the test cases (presented in Ait Ouméziane 2011) enable to begin the simulation of a full scale experiment of hemp concrete wall behaviour.

3. Experimental setup and material data

3.1 Description of the hemp concrete wall

A laboratory experiment is performed to evaluate at full scale the behaviour of a hemp concrete wall submitted to different climatic solicitations. For that purpose a mixed wall built with 31 blocks of hemp concrete and wood elements stands

as the wall of separation between two climatic rooms (figure 1). Blocks are cast from moulds which are 60 cm long, 30 cm wide and 30 cm high. The climatic rooms simulate interior and exterior climate.

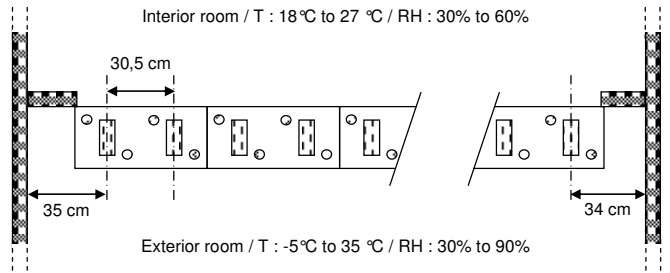


Fig. 1. Wall configuration

In order to describe temperature and relative humidity variations, several humidity sensors and thermocouples have been put inside the wall, at wall surfaces and in both surroundings. The created gaps for sensors putting are chosen in order to limit the effect on one dimensional mass and heat transfer. The acquisition system collects the measures every five minutes. In this paper, a block in the middle of the wall is studied. The positions of the sensors for that particular block are described in figure 2.

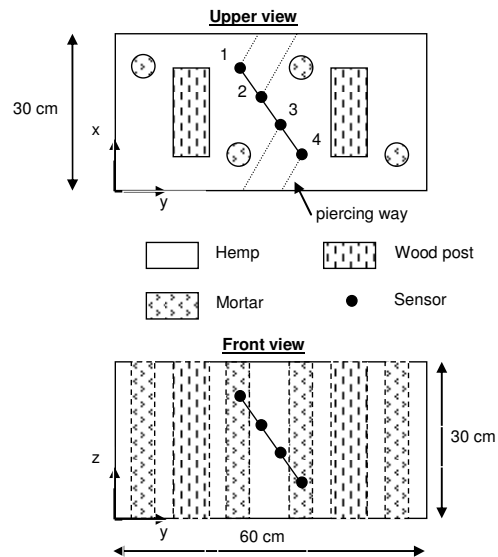


Fig 2. Hemp concrete block ($x_1 = 0.22$ m, $x_2 = 0.18$ m, $x_3 = 0.12$ m and $x_4 = 0.08$ m)

3.2 Climatic variations

Different sequences of climatic solicitations have been carried out to study the hemp concrete wall behaviour. In this paper one almost isothermal sequence is presented.

Before the beginning of each test, the wall is stabilized at 40% and 23°C by keeping constant exterior and interior humidity and temperature during the appropriate period. In the studied cases the temperature is set to 23°C for both sides of the wall, the interior relative humidity is set to 40% and the exterior relative humidity varies between 50% and 80%. The measured external and internal temperatures and relative humidity are presented in figure 3. The sequence lasts two weeks.

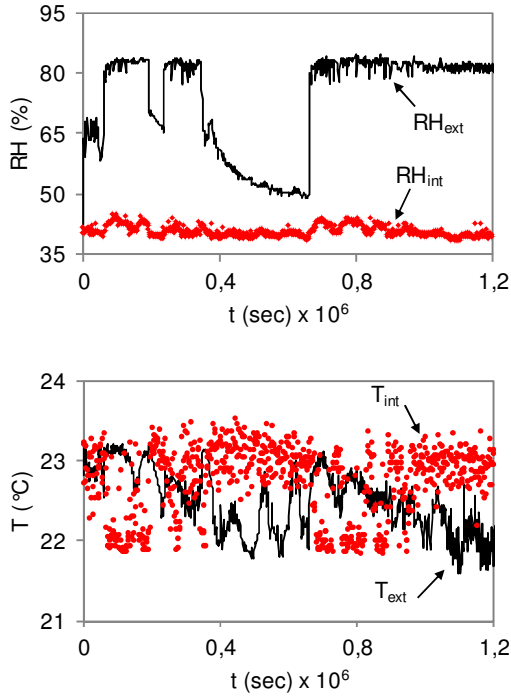


Fig. 3. Exterior and interior relative humidity and temperature.

3.3 Properties of the hemp concrete

In the frame of industrial collaboration properties of hemp concrete are obtained from a set of experiments performed in our laboratory (Chamoïn 2011, Collet 2008). The density of the dry material is $\rho_0 = 420 \text{ kg.m}^{-3}$. The specific heat capacity of the dry material is $C_0 = 1000 \text{ J.kg}^{-1}.\text{K}^{-1}$. Considering the range of relative humidity encountered by the material in the experimental sequences, between 40%RH and 80%RH, the heat conductivity can be taken as constant $\lambda = 0.15 \text{ W.m}^{-1}.\text{K}^{-1}$.

The sorption characteristics are given by measurement of water content at relative humidity of 11%, 23%, 33%, 43%, 58%, 81%, 90%, 95% and 97%. Hemp concrete presents a hysteresis between the main wetting curve and the main drying curve (figure 4).

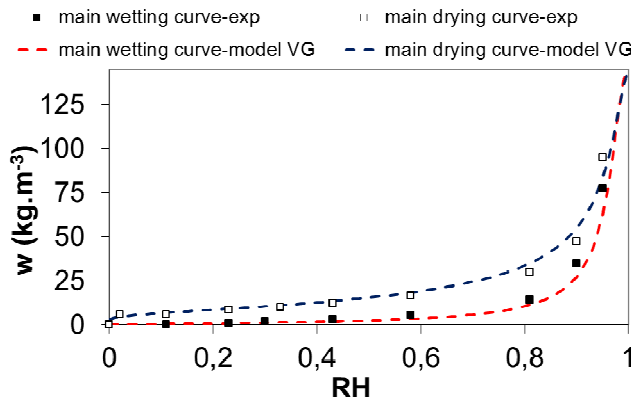


Fig. 4. Main wetting and drying curves: experimental points and models

The Van Genuchten model is used to model the main drying and wetting curves:

$$w = w_{sat} \left(1 + \left| \alpha_j \frac{RT_{ref}}{M_w g} \ln(\phi) \right|^{\eta_j} \right)^{\frac{1}{\eta_j - 1}}, \quad j = ads \text{ or } des \quad (12)$$

where w_{sat} is the saturated water content and the indexes α_j and η_j are parameters to be determined for the main drying curve (des for desorption) and the main wetting curve (ads for adsorption) thanks to experimental data. The fitted parameters are $\alpha_{ads} = 0.0024$, $\alpha_{des} = 0.0026$, $\eta_{ads} = 2.3$ and $\eta_{des} = 1.694$.

The water vapour permeability is measured experimentally by the wet cup method. Four couples of humidity are used: 0-23%, 43-58%, 58-81% and 81-90%. This set of data allows the determination of apparent water vapour permeability since in such experiment the actual moisture flow involves both liquid and vapour transport. Because each specimen is dried at the beginning of the cup test, the results can be presented as function of the water content as in figure 5.

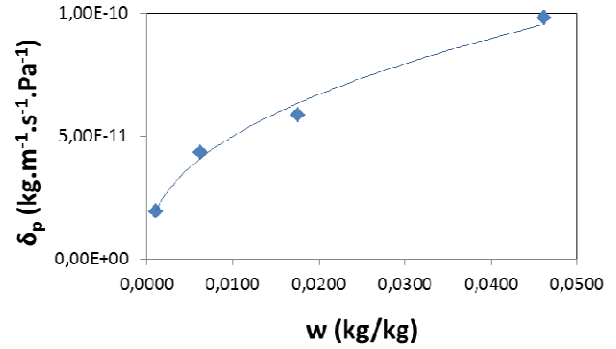


Fig. 5. Vapour permeability in function of the water content taken on the main wetting curve

The variation of this apparent water vapour permeability with water content is described by the following power law (with a correlation coefficient $R^2 = 0.994$):

$$\delta_p = 3.67 \times 10^{-10} (w_{ads})^{0.488} \quad (11)$$

3.4 Boundary conditions

In this case, no air transfer is present since there is no pressure gradient between the two climatic rooms. The heat transfer boundary coefficient is derived from the hypothesis of an isothermal plane plate. The mass surface coefficient is determined with the Lewis relation. The resulting values respectively for h and β are about $6 \text{ W.m}^{-2}.\text{K}^{-1}$ and $4.10^{-8} \text{ s.m}^{-1}$.

4. Hysteresis modelling

Studies of Van Belleghem (2010), Steeman (2009) or Kwiatkowski (2009) showed the influence of sorption hysteresis on water vapour transfer in building construction materials. In a recent work (Ait Oumeziane 2011) similar trends have been observed in hemp concrete. Indeed, the main wetting/drying isotherms used as boundary curves do not describe the real evolution of water content in current use. Due to hysteresis effect, water content for a given relative humidity is between the values given by wetting and drying curves depending on the previous variations of the material. The water content is not only under or overestimated according to the choice of wetting or drying curve but above all its storage capacity is in each case widely overestimated. In Ait Oumeziane (2011), an over-simplified modelling of hysteresis effect based on rough evaluation of intermediate scanning curves was presented. In the present

work an improved modelling of the scanning curves is investigated.

Apart from the empirical model of Pedersen (1990) kind there are globally two main groups of hysteresis models in the literature (Lehmann 1998):

- The physical model (Mualem group)
- The mathematical model (Kool & Parker group)

The first group explains the shape of the scanning curve by means of physical properties such as the distribution of the pore radii (Mualem 1974). The second group describes the scanning curves with expressions similar to the main drying and wetting curves, assuming the same curve shape parameters (Kool and Parker 1987). In the present work the use of the Huang model (Huang 2005) based on the Kool&Parker group is proposed.

4.1 The KP modelling

The scanning curves follow the same form as the main drying and wetting curves. Huang (2005) proposes for main curves the Van Genuchten model and the i^{th} scanning curve also writes:

$$w(\varphi) = w_r(i) + (w_s(i) - w_r(i)) \left(1 + \left| \alpha \frac{RT_{ref}}{M_w g} \ln(\varphi) \right|^\eta \right)^{\frac{1}{\eta} - 1} \quad (13)$$

where the indexes α and η are parameters issued for the main drying curve expression or the main wetting curve expression, $w_r(i)$ and $w_s(i)$ represents respectively the residual and the saturated water contents for i^{th} scanning curve.

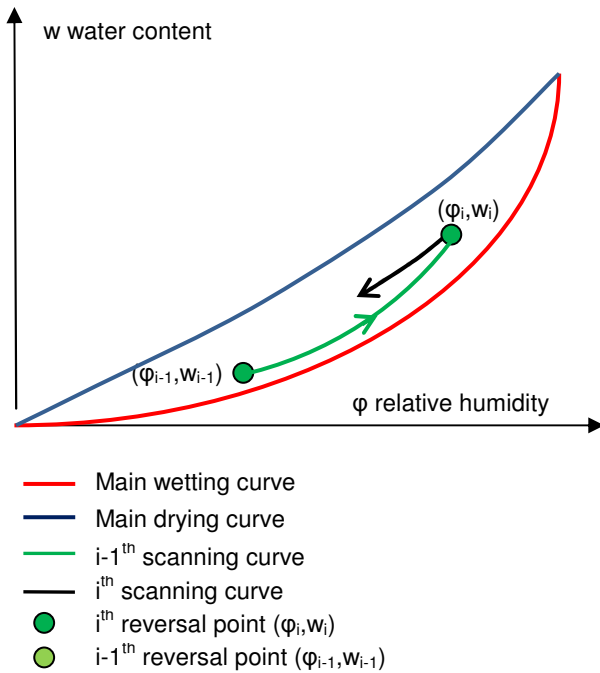


Fig. 6. Schematic representation of construction of the i^{th} drying curve

Huang (2005) notes that the term into brackets in eq. (13) is the same for all scanning curves. So, the determination of the i^{th} curve is only based on the parameters $w_r(i)$ and $w_s(i)$. Each i^{th} scanning curve includes the last reversal point (φ_i, w_i) and

the penultimate reversal point too (φ_{i-1}, w_{i-1}) (see figure 6). Determining $w_r(i)$ and $w_s(i)$ consists in solving a linear system of two equations.

This model implemented in Matlab enhances the formulation of the 1D HAM model described in the second section.

5. Hemp concrete wall without coating

In this section, the model results are confronted to the experimental data obtained on the hemp concrete wall submitted to the previously presented climatic solicitations (see figure 3).

In order to ensure graph readability, the results focus on one unique sensor at $x_4 = 8$ cm, the nearest position from the exterior side of wall. The whole results will be dealt subsequently.

5.1 Influence of the hygrothermal properties

The influence of material property is numerically tested by applying 10% variation to heat capacity and heat conductivity and apparent water vapour permeability. Variations in heat capacity or heat conductivity show no significant impact on the relative humidity and temperature evolutions.

A larger effect is observed on relative humidity when applying variation of the apparent vapour permeability. However as can be seen on figure 7, the influence is quite small leading to the conclusion that the variations of these parameters due to measurement uncertainty are negligible for the present purpose.

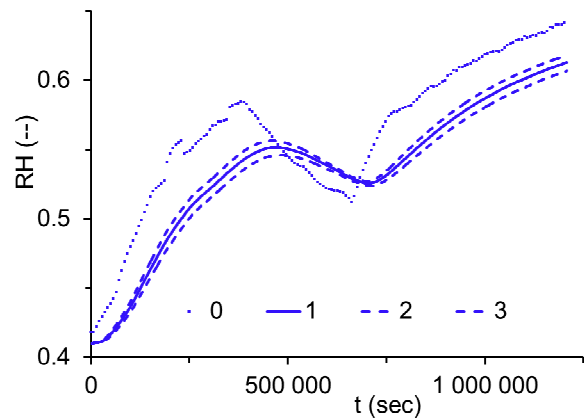


Fig. 7. Sensibility of the apparent water vapor permeability on the distribution of the relative humidity at the depth $x_4 = 8$ cm (0: experimental points, 1: $\delta p(w_{ads})$, 2: $\delta p(w_{ads}) + 10\%$ and 3: $\delta p(w_{ads}) - 10\%$)

5.2 Influence of the sorption isotherm

The influence of sorption modelling on the distribution of relative humidity is presented in figure 8. The following modelling solutions are evaluated:

- 0: experimental points
- 1: sorption isotherm following the main wetting curve (continuous blue line)
- 2: sorption isotherm following the main drying curve (dotted green line)

- **3:** sorption isotherm following the average of the main wetting and the main drying curves (dotted yellow line)
- **4:** sorption isotherm governed by the hysteresis model of Huang (dotted red line). For this model, the first scanning curve corresponds to the main wetting curve.

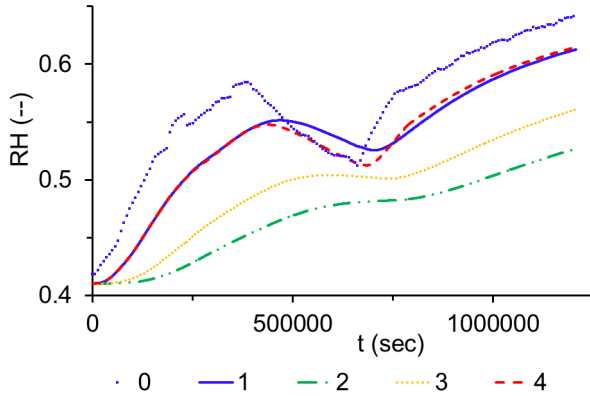


Fig. 8. Distribution of relative humidity at the depth $x_4 = 8$ cm for different sorption modelling

First it appears clearly that the curves 2 and 3 are not suited to represent the measured hydric behaviour of the hemp concrete. The use of the drying curve or the average curve leads to an over-estimation of the hydric capacity acting as a retarder to moisture penetration.

Simulations using the curve 1 or the curve 4 lead to underestimation of measured relative humidity of about 5%. Such results are quite satisfactory considering both sensors measurement uncertainty (about 2%RH) and sensors position uncertainty (as described in next part). The main difference between the two modelling is observed during the drying phase (t between $4 \cdot 10^5$ s and $6 \cdot 10^5$ s). During this period the hysteresis model use an intermediate scanning curve to describe the material humidity storage. This leads to a reduced value of the hydric capacity of the material when compared to the use of the main wetting curve. During the first wetting phase (t about $4 \cdot 10^5$ s), the scanning curve from the hysteresis model is the main wetting curve because initial water content is taken on the main wetting curve, see paragraph 2.5.2. That is why the results are exactly the same during this phase.

The main wetting curve appears in that case to be a satisfactory approximation for moisture storage. However during drying stages the use of hysteresis modelling enable an enhanced representation of moisture storage in the material. Hysteresis modelling is adopted for the following simulation results.

5.3 Influence of the sensor positions

The present section focuses on the influence of sensor position on the presented results. The size of the head of the humidity sensors is approximately of 5 mm. Moreover the installation of the sensors inside the wall required to pierce the wall in an oblique direction (see section 3.1). Considering these two parameters the uncertainty on the position of the

sensors is estimated to ± 1 cm. Figure 9 gives the simulations results for $x_1 = 22$ cm ± 1 cm and $x_4 = 8 \pm 1$ cm.

A larger effect is observed for the sensor next to the surrounding submitted to relative humidity steps. For this sensor a 1cm variation in the position provides a better fitting with experimental data. In the case of the sensor next to the surrounding submitted to constant relative humidity the sensor position uncertainty shows no relevant influence. In both cases differences between numerical and experimental results are in the range of the sensors uncertainty (about 2%RH).

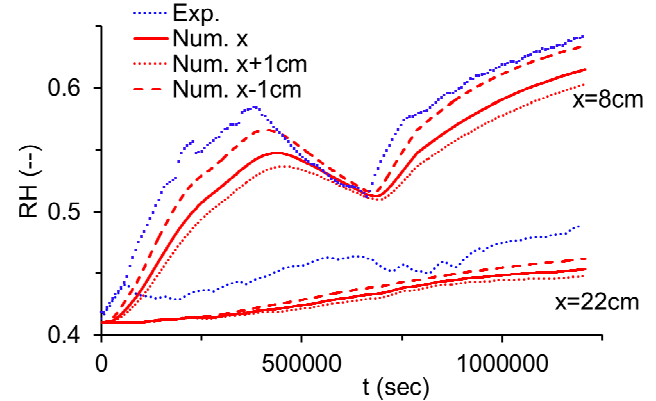


Fig. 9. Distribution of relative humidity at the depths $x_1 = 22 \pm 1$ cm and $x_4 = 8 \pm 1$ cm

5.4 Conclusion on the modelling

Results of relative humidity distributions including hysteresis modelling are presented in figure 10 for all the depths. In figure 11 two depths only are presented for the temperature distribution in order to ensure the graph readability.

A good agreement between simulation results and experiment is achieved for the temperatures. Considering the different uncertainties developed previously, at which the uncertainties linked to the evaluation of the hygrothermal properties could be added, the results got for the relative humidity distribution through the material seems acceptable. The hysteresis model of Huang is able to describe physically the real hydric behaviour of the hemp concrete. Moreover, during successive periods of wetting and drying and particularly with high change (for example at the scale of the year), hysteresis models give a better evaluation of the hydric capacity which stays the sensitive parameter of the relative humidity distribution through a porous wall.

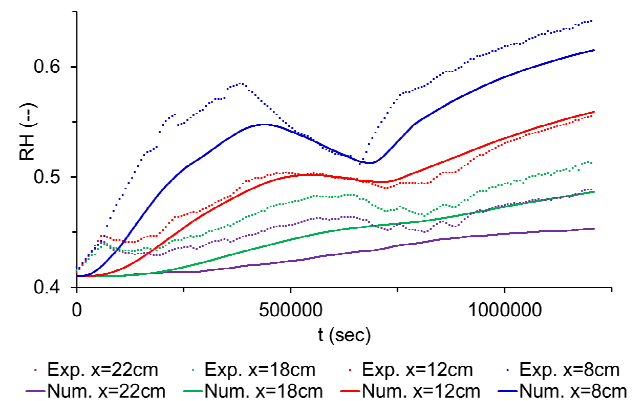


Fig. 10. Experimental (dashed lines) and simulated (continuous lines) relative humidity for different depths

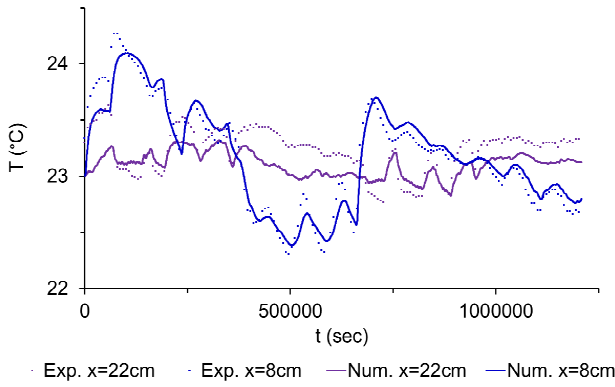


Fig. 11. Experimental (dashed lines) and simulated (continuous lines) temperature for two depths

6. Hemp concrete wall with coating

In this section, a coated wall is investigated numerically. The case study consists of a 30 cm hemp concrete wall covered on one side with hemp lime coating. Two coating thicknesses are analysed and compared : 5cm and 3 cm.

6.1 Coating properties

The hemp lime coating properties are issued from Collet (2004) : the density of the dry material $\rho_0 = 785 \text{ kg.m}^{-3}$, the heat conductivity $\lambda = 0.28 \text{ W.m}^{-1}.\text{K}^{-1}$, the specific heat capacity $C_0 = 1070 \text{ J.kg}^{-1}.\text{K}^{-1}$ and the vapour permeability $\delta_p = 2.10^{-11} \text{ kg.m}^{-1}.\text{s}^{-1}.\text{Pa}^{-1}$. Available measurements for water vapour permeability allow neglecting the influence of water content for hemp lime coating.

The sorption characteristics are given by the discrete values obtained from experiment (water content at relative humidity of 23%, 48%, 58%, 81% and 97%). As hemp concrete, the hemp/lime coating presents a hysteresis between main adsorption and main desorption (figure 12).

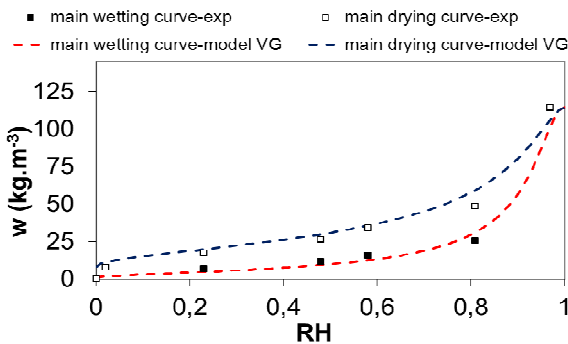


Fig. 12. Main wetting and drying curves: experimental points and models.

Hysteresis is described by Huang model and Van Genuchten formalism is used (see eq. 12) with the fitted parameters $\alpha_{\text{ads}} = 0.0012$, $\alpha_{\text{des}} = 0.009$, $\eta_{\text{ads}} = 2$ and $\eta_{\text{des}} = 1.6$

6.2 Climatic variations

For the numerical test, temperatures remain constants equal to 23°C and the side with coating is submitted to 4 steps in relative humidity. Hydric solicitations are presented in figure 13.

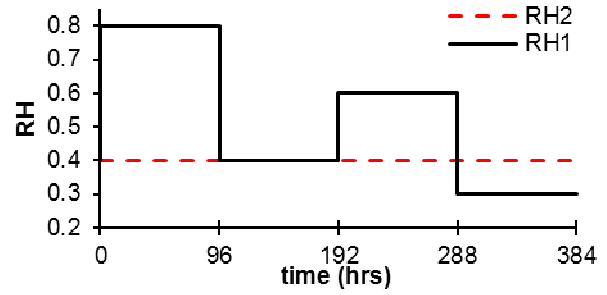


Fig. 13. Hydric solicitations for the numerical test.

6.3 Numerical results

6.3.1 Coating effect RH versus time

Relative humidity evolution for hemp concrete at 22 cm and 8 cm are presented in figure 14. In the following discussion the emphasis is on relative humidity distributions next to the boundary submitted to steps changes ($x = 8 \text{ cm}$).

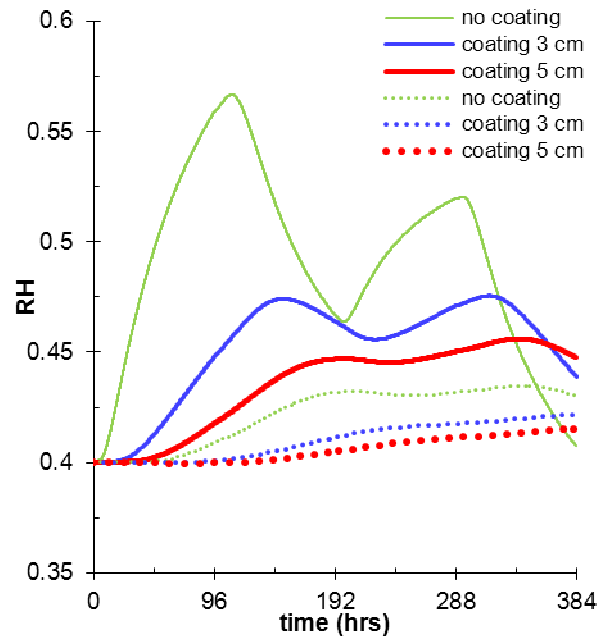


Fig. 14. Relative humidity evolution for hemp concrete without coating, with 3 cm coating and with 5 cm coating at $x_1 = 0.22 \text{ m}$ (dashed lines) and $x_4 = 0.08 \text{ m}$ (lines).

As expected coating plays a part in limiting moisture diffusion in hemp concrete : $\phi_{\text{max}} = 0.57$ without coating, $\phi_{\text{max}} = 0.47$ with 3 cm coating and $\phi_{\text{max}} = 0.45$ with 5 cm coating. According to figure 14, the kinetic during wetting and drying stages is slow down due to coating. After each step in boundary relative humidity the maximum or minimum values of relative humidity in the coated wall are reached with delay when compared to wall without coating. Table 1 resumes the time of the occurrence of these extrema for $x = 8 \text{ cm}$.

Table 1. Coating effect on maximum wetting or drying time occurrence

| | No-coating | 3cm coating | 5cm coating |
|------------------------------|------------|-------------|-------------|
| 1 st max. wetting | 110 hrs | 150 hrs | 198 hrs |
| 1 st max. drying | 200 hrs | 225 hrs | 234 hrs |
| 2 nd max. wetting | 300 hrs | 324 hrs | 339 hrs |

Finally, almost the same damping effect is observed with 3 cm and 5 cm coating.

6.3.2 Coating effect RH versus wall thickness

The following figures present relative humidity distributions 12 hours and 96 hours after a sudden change in climatic variations, respectively 80%RH, 40%RH, 60%RH and 30%RH.

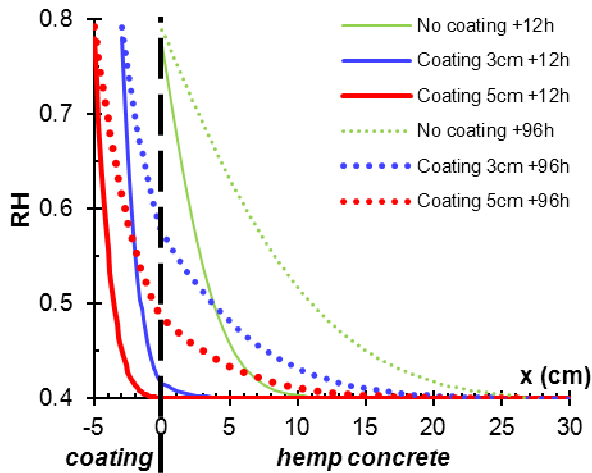


Fig. 15. Relative humidity distributions at 12 hours and 96 hours after RH_1 assigned to 80%

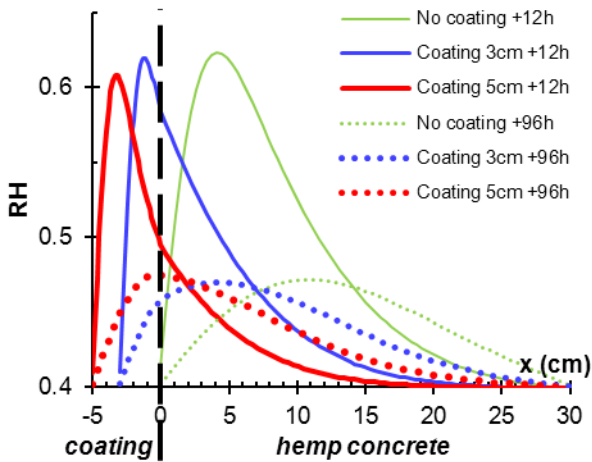


Fig. 16. Relative humidity distributions at 12 hours and 96 hours after RH_1 assigned to 40%

For a period of 12 hours after a wetting stage (figure 15 and 17) coating restricts hemp concrete wetting. In the same way, for a period of 12 hours after a drying stage (figure 16 and 18) coating restricts hemp concrete drying. In these last cases the first few centimeters of hemp concrete under the coating are subject to higher relative humidity levels for coated wall than for wall without coating.

For a long period of 96 hours (4 days) after wetting or drying stages coating releases moisture in the hemp concrete.

Finally each wall configuration leads to almost similar response when looking at the behaviour of the first 10 cm of material (either hemp lime and hemp concrete or hemp concrete only) in contact with the surrounding submit to step change in relative humidity. Thus hemp lime coating is not a vapour barrier but rather a moisture buffer able to release

humidity for longer times. Finally, in the case of the proposed climatic variations, the coating thickness provides no significant difference on moisture distribution.

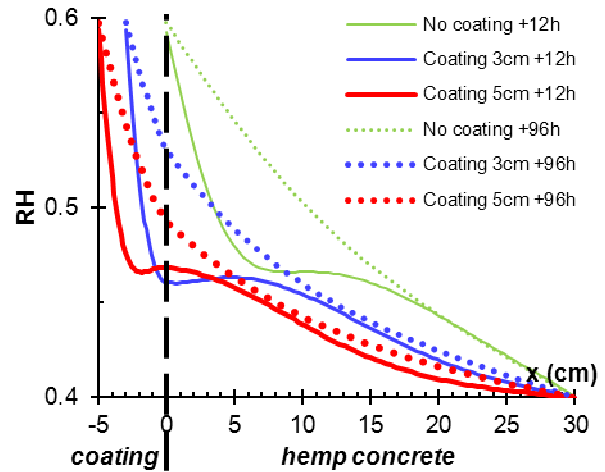


Fig. 17. Relative humidity distributions at 12 hours and 96 hours after RH_1 assigned to 60%

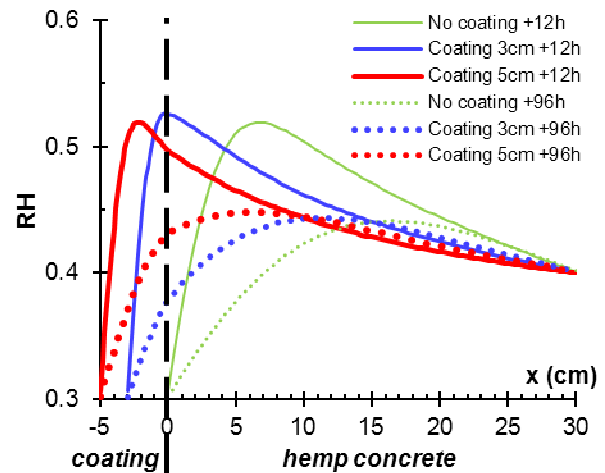


Fig. 18. Relative humidity distributions at 12 hours and 96 hours after RH_1 assigned to 30%

7. Conclusion

This paper provides some indications regarding the hygrothermal behaviour of hemp concrete with and without coating. For this material, taking into account the hysteresis of the sorption isotherms appears to be a determinant factor for the modelling of drying stages. This fact has to be confirmed by comparing the numerical results to different experimental cases namely some with successive drying and wetting stages.

Two hemp lime coating thickness (5 cm or 3 cm) were investigated numerically in the present work. This initial work about coating confirms expected result concerning both the moisture buffering effect of hemp lime coating for short time and moisture redistribution in hemp concrete for long time. This kind of coating, whatever its thickness, preserves the breathing properties of hemp concrete wall.

The coating thickness optimization is a real challenge both for obvious economic reasons and in the sustainable context for reducing the carbon impact due to lime. This aspect of the

work will be continued in a numerical and experimental ways. For that purpose a set of experiments has been launched recently in the laboratory on the hemp concrete wall coated with hemp-lime coating. Results obtained regarding hydrothermal transfer with traditional lime mortar renders will be compared with present results.

Although the presence of wood and gaps in the wall induces a full 3D transfer problem, the simulation was here carried out in 1D. This simplification is a tough one: if the wood posts can reasonably be supposed not disturbing the transfers through the particular block studied, the presence of network gap is certainly of importance. The experimental setup should be able to answer the question of 3D effects since sensors have been placed in various wall blocks.

Acknowledgements

The authors acknowledge financial support of French Research Agency (ANR) and Region Bretagne for experimental part of this work, within the frame of the projects BETONCHANVRE ANR-06-MAPR-0002 and PRIRECOMATX 2005.

References

- Ait Oumeziane Y., Bart M., Moissette S., Lanos C., Prétot S., Collet F. 2011. Hygrothermal behaviour of a hemp concrete wall : influence of sorption isotherm modelling. in : Proceedings of the 9th Nordic Symposium on Building Physics (NSB 2011), Tampere, Finland, May 29-June 2, 2011
- Ait Oumeziane Y. Bart M. Moissette S. Lanos C. 2011. Modélisation du transfert d'air, de masse et de chaleur aux travers de parois multicouches. In Proceedings of the X^{ème} Colloque Interuniversitaire Franco-Québécois (CIFQ2011), Chicoutimi, Canada, June 20-22, 2011
- Collet F. 2004. Caractérisation hydrique et thermique de matériaux de génie civil à faibles impacts environnementaux, PhD thesis
- Collet F. Bart M. Serres L. Miriel J. 2008, Porous structure and water vapour sorption of hemp-based materials. Construction and Building Materials 22, p. 1271-1280.
- Evrard A. 2008. Transient hygrothermal behaviour of Lime-Hemp Materials. PhD-Thesis, Université Catholique de Louvain, Belgium.
- Hagentoft C.E, Kalagasidis A.S, Adl-Zarrabi B, Roels S, Carmeliet J, Hens H, Grunewald J, Kunk M, Becker R, Shamir D, Adan O, Brocken H, Kumaran K, Djebbar R. 2004, Assessment Method for Numerical Prediction Models for Combined Heat, Air and Moisture Transfer in Building Components: Benchmarks for One-dimensional Cases, Journal of Thermal Envelope and Building Science 27(4), p. 327-352.
- Huang H-C., Tan Y-C, Liu C-W, Chen C-H, 2005, A novel hysteresis model in unsaturated soil, Hydrological Processes, vol. 19, issue 8, p. 1653-1665.
- Kwiatkowski J., Woloszyn M., Roux J.-J. 2009, Modelling of hysteresis influence on mass transfer in building materials. Building and Environment 44, p. 633-642.
- Kool J.B. and Parker J.C. 1987. Development and evaluation of closed form expressions for hysteretic soil hydraulic properties, Water Resources research, Res. 23, p.105-114
- Kunzel H. M. 1995. Simultaneous heat and moisture transport in building components, Fraunhofer IRB Verlag Stuttgart, Germany

Lehmann P., Stauffer F., Hinz C., Dury O., Flühler H. 1998. Effect of hysteresis on water flow in sand column with a fluctuating capillary fringe. Journal of Contaminant Hydrology 33, p.81-100.

Mualem Y. 1974. A conceptual model of hysteresis, Water Resources research, vol 10, n°3, p.514-520

Pedersen C.R. 1990. Transient calculation on moisture migration using a simplified description of hysteresis in sorption isotherms, The 2nd symposium on building physics in the Nordic Countries, Trondheim, 20-22 August 1990

Samri D. 2008. Analyse physique et caractérisation hygrothermique des matériaux de construction: approche expérimentale et modélisation numérique,. PhD-Thesis, Institut National Sciences Appliquées de Lyon, France.

Steeman H.-J., Van Belleghem M., Janssens A., De Paepe M. 2009, Coupled simulation of heat and moisture transport in air and porous materials for the assessments of moisture related damage. Building and Environment 44, p. 2176-2184.

Van Belleghem M, Steeman H.-J., Steeman M., M., Janssens A., De Paepe M. 2010, Sensitivity analysis of CFD coupled non-isothermal heat and moisture modelling. Building and Environment 45, p. 2485-2496.